AD-A209 859

ATIC FILE COPY

④

A Raman Spectral Study of the Equilibria of Zinc Bromide Complexes in DMSO Solutions

by

DTIC COPY INSPECTED 1

J. van Heumen, T. Ozeki, and D.E. Irish

Prepared for Publication

in

Canadian Journal of Chemistry

Accession For

NTIS GRA&I	☒
DTIC TAB	☐
Unannounced	☐
Justification

By

Distribution/

Availability Codes

| Dist | Avail and/or Special |
| A-1 | |

Guelph-Waterloo Center for Graduate Work in Chemistry
Waterloo, Campus
Department of Chemistry
University of Waterloo
Waterloo, Ontario
Canada, N2L 3G1

DTIC
ELECTE
JUL 0 5 1989
S E D
Cb

June 13, 1989

89 7 05 063

REPORT DOCUMENTATION PAGE

1a. REPORT SECURITY CLASSIFICATION	1b RESTRICTIVE MARKINGS
Unclassified	

2a. SECURITY CLASSIFICATION AUTHORITY	3 DISTRIBUTION/AVAILABILITY OF REPORT
Unclassified	
2b DECLASSIFICATION/DOWNGRADING SCHEDULE	Public Release/Unlimited

4. PERFORMING ORGANIZATION REPORT NUMBER(S)	5. MONITORING ORGANIZATION REPORT NUMBER(S)
ONR Technical Report #4	

6a NAME OF PERFORMING ORGANIZATION	6b. OFFICE SYMBOL (If applicable)	7a NAME OF MONITORING ORGANIZATION
D. E. Irish University of Waterloo		Office of Naval Research

6c ADDRESS (City, State, and ZIP Code)	7b ADDRESS (City, State, and ZIP Code)
Department of Chemistry University of Waterloo Waterloo, Ontario, Canada, N2L 3G1	The Ohio State University, Research Center 1314 Kinnear Road, Room 318 Columbus, Ohio, U.S.A., 43212-1194

8a NAME OF FUNDING/SPONSORING ORGANIZATION	8b OFFICE SYMBOL (If applicable)	9 PROCUREMENT INSTRUMENT IDENTIFICATION NUMBER
Office of Naval Research		N00014-87-J-1118

8c ADDRESS (City, State, and ZIP Code)	10 SOURCE OF FUNDING NUMBERS			
Chemistry Division 800 N. Quincy Street Arlington, VA, U.S.A., 22217-5000	PROGRAM ELEMENT NO.	PROJECT NO	TASK NO	WORK UNIT ACCESSION NO

11 TITLE (Include Security Classification)
A Raman Spectral Study of the Equilibria of Zinc Bromide Complexes in DMSO Solutions (unclassified)

12 PERSONAL AUTHOR(S)
J. van Heumen, T. Ozeki, and D.E. Irish

13a TYPE OF REPORT	13b TIME COVERED	14. DATE OF REPORT (Year, Month, Day)	15. PAGE COUNT
Technical	FROM 08/88 TO 06/89	1989-06-13	26

16. SUPPLEMENTARY NOTATION

Submitted to the Canadian Journal of Chemistry

17. COSATI CODES			18 SUBJECT TERMS (Continue on reverse if necessary and identify by block number)
FIELD	GROUP	SUB-GROUP	zinc bromide complexes; solvation in DMSO; Raman spectroscopy; factor analysis, thermodynamics; metal complexes. (KT)

19 ABSTRACT (Continue on reverse if necessary and identify by block number)

Using Raman spectroscopy, the stepwise formation of zinc bromide complexes in dimethylsulfoxide (DMSO) solution has been investigated. The presence of four different zinc-bromide complexes is suggested and their Raman spectra have been extracted. The formation constant of each reaction has been estimated by the application of factor analysis to the spectra. The usual methods of factor analysis have been extended by the introduction of constraints imposed by the equilibria.

20. DISTRIBUTION/AVAILABILITY OF ABSTRACT	21. ABSTRACT SECURITY CLASSIFICATION
☒ UNCLASSIFIED/UNLIMITED ☐ SAME AS RPT. ☐ DTIC USERS	Unclassified

22a. NAME OF RESPONSIBLE INDIVIDUAL	22b. TELEPHONE (Include Area Code)	22c. OFFICE SYMBOL
Dr. Robert J. Nowak	(519) 885-1211, ext. 2500	

DD FORM 1473, 84 MAR
83 APR edition may be used until exhausted.
All other editions are obsolete.

A Raman spectral study of the equilibria of zinc bromide complexes in DMSO solutions.

Jeff van Heumen, Toru Ozeki[*] and Donald E. Irish

Department of Chemistry, University of Waterloo, Waterloo, Ontario, Canada N2L 3G1.

[*] Present address: *Hyogo University of Teacher Education, 942-1 Shimokume, Yashiro-cho, Kato-gun, Hyogo, Japan 673-14*

ABSTRACT

Using Raman spectroscopy, the stepwise formation of zinc bromide complexes in dimethylsulfoxide (DMSO) solution has been investigated. The presence of four different zinc- bromide complexes is suggested and their Raman spectra have been extracted. The formation constant of each reaction has been estimated by the application of factor analysis to the spectra. The usual methods of factor analysis have been extended by the introduction of constraints imposed by the equilibria.

KEY WORDS: zinc bromide complexes; solvation in DMSO; Raman spectroscopy; factor analysis.

INTRODUCTION

Professor Ronald J. Gillespie has had a long standing interest in the shapes of complexes and molecules. It is a pleasure to dedicate this article to him on the occasion of his 65 th birthday.

Ahrland and co-workers have reported the results of detailed studies of metal complex formation between Group IIB metals and halide ions in the dipolar aprotic solvent, dimethylsulfoxide (DMSO) (1-9). Emphasis was placed on the thermodynamics of the stepwise equilibria and evidence for structural changes between successive complexes. The solvent, DMSO has been investigated quite extensively as a neat liquid (10-12), and as a solvent in which complex formation occurs. The complexes are more stable in DMSO than in water because the former has a lower dielectric constant (1,3,9). The uncomplexed metal cations — zinc, cadmium or mercury — are believed to exist as octahedral species, the ions being solvated via oxygen by six DMSO molecules (6,13,14). However evidence suggests that their coordination symmetry changes from six-coordinate octahedral to four-coordinate tetrahedral as higher halide complexes are formed. Enthalpy and entropy values for the cadmium halide system suggest that a coordination change occurs at the second step of complex formation: a step from $CdBr^+$ to $CdBr_2$ (2). For the zinc bromide complexes Ahrland et al. have suggested the possibility that the change occurs at the first step of complex formation in 1M NH_4ClO_4 media: a step from Zn^{2+} to $ZnBr^+$ (4). In a succeeding paper (7), they reported that the step giving rise to the coordination change depends upon the co-existing salt and ionic strength of the solution, such that this change in coordination of the zinc bromide complex might occur at the second step in 0.1M

NH_4ClO_4 media. Several other methods such as NMR (15,16) and X-ray diffraction (17) have also been used to study this kind of phenomenon. All reports support the view that the complex finally formed — $ZnBr_4^{2-}$ or $CdBr_4^{2-}$ — is a tetrahedral complex.

Raman spectroscopy is a useful tool for investigation of the structure of these complexes because the latter have Raman active vibrational modes (18-21); and the technique is, in principle, capable of providing information about their geometry. From the Raman intensities information about the concentrations of each species can be obtained and hence the stability and equilibrium constants can be estimated. This work was undertaken to complement recent studies of zinc and cadmium bromide complexes in water (20, 21) and to extend those works to nonaqueous solutions. This work is focussed on zinc bromide complex formation in DMSO solutions, especially on the determination of the stepwise stability constants and the stage at which the coordination change takes place.

EXPERIMENTAL

Nine solutions were prepared by dissolving given amounts of zinc bromide (J.T. Baker, "Baker Analyzed") $ZnBr_2$ and different amounts of sodium bromide (BDH, Laboratory Reagent) NaBr in solvent DMSO (BDH, Analytical Reagent) $SO(CH_3)_2$. In order to prepare solutions with different R values (the molar ratio of total bromide to total zinc) sodium bromide was added. In the case of R < 2.0, zinc perchlorate (GFS Chemicals) $Zn(ClO_4)_2 \cdot 6H_2O$ was used in place of sodium bromide. The introduction of a small amount of water is not expected to introduce a serious problem as DMSO solvates zinc(II) much more strongly than water does (5,9). R values of the sample solutions and their compositions are given in Table 1.

Concentrations are given in mol kg^{-1} of DMSO.

Samples were placed in glass capillary tubes for Raman measurements. To avoid solvent evaporation the open end of the capillary was flame-sealed. All spectra were collected at a temperature of 25°C by using a thermostatted capillary tube holder.

Raman spectra were recorded using a Jarrell-Ash 25-100, 1.0 meter Czerny-Turner monochromator equipped with a digital cosecant stepping drive, an RCA 31034 selected photomultiplier tube, and an SSR model 1105/1120 photon counting system. Spectra were excited by the 514.5 nm line of a Spectra-Physics Ar$^+$ Laser, Model 165, operating at a power of 1400 mW. The spectrometer was interfaced to Commodore-Pet Model 2001 and 2040 computers. The digitized data were also analyzed by the DEC-PRO 380 and VAX 11/785 computers, using procedures such as spectral band fitting, exponential baseline correction, and factor analysis.

RESULTS AND DISCUSSION

Four spectral regions; a) 260 to 420 cm^{-1}, b) 800 to 1150 cm^{-1}, c) 600 to 750 cm^{-1} and d) 150 to 230 cm^{-1} are considered below.

a) 260 to 420 cm^{-1} region of the Raman spectra.

This region, shown in Figure 1, contains the symmetric and the antisymmetric deformation bands of the carbon-sulfur-oxygen bond at 382 and 333 cm^{-1} respectively, as well as a carbon-sulfur-carbon deformation band at 305cm^{-1}. No additional bands were observed and the three bands showed no significant change in band shape with the change in R value.

b) 800 to 1150 cm^{-1} region of the Raman spectra.

The bands of this region arise from the sulfur-oxygen vibration of DMSO. Figure 2 illustrates the effect of complexing on the sulfur-oxygen vibration of the DMSO molecule as the R value

increases. Solid lines are the Raman spectra of each sample and dotted lines show the spectra of neat DMSO. Sharp peaks observed at 930 cm^{-1} for R=1.0 and 1.5 samples correspond to the $v_1(a_1)$ symmetrical stretching vibration of perchlorate ion. The shaded area between the solid and the dotted lines indicates the difference between the spectrum of the neat solvent and that of the sample solution; it arises from the perturbed sulfur-oxygen bond, resulting from the solvation by DMSO molecules of the zinc cation (cf. Ref.6). The decrease in the shaded area suggests the decrease in the amount of DMSO solvating the zinc cation as the bromide concentration increases. The sulfur-oxygen stretching band, seen in Fig.2 at 1042 cm^{-1}, provides indirect information for the zinc-DMSO bonding. If some interaction occurs between zinc cation and oxygen of the DMSO molecule, the metal cation will attract the electron cloud of the sulfur-oxygen bond, and as a result reduce the bond order of the sulfur-oxygen bond. Consequently, the vibrational energy will be lowered and the Raman band position will shift to a lower wavenumber. The evidence for this shift is clearly seen at R=1 in Fig.2; a new band appears at 1017 cm^{-1} (1021 cm^{-1} in the solid solvate (6)). On increasing the R value, obviously there is seen a decrease in the intensity of this new band. At R=3.2, the new peak no longer exists. This fact is interpreted as desolvation of DMSO from the solvation sphere of the zinc cation to the free bulk state.

c) 600 to 750 cm^{-1} region of the Raman spectra.

This wavenumber region is dominated by a symmetric stretching band at 670 cm^{-1} and an antisymmetric stretching band at 700 cm^{-1}, both due to the carbon-sulfur bonding in the DMSO molecule. Figure 3 provides comparison of the Raman spectra of the neat DMSO (dotted lines) and the DMSO/Zn^{2+}-Br^- mixtures (solid lines). The shaded area between the two spectra indicates the difference between the

spectrum of the neat solvent and that of the sample solution. At
the lowest R value, R=1.0, two additional peaks appear at higher
wavenumbers, 681 and 714 cm^{-1} (683 and 717 cm^{-1} in the solid solvate
(6)). As described in the previous section the solvation of zinc
ion by DMSO molecules reduces the bond order of the sulfur-oxygen
bond. This may cause the adjacent carbon-sulfur bond to aquire
extra electron density and its bond strength to increase. As a
matter of fact, the peak wavenumber of the carbon-sulfur vibration
shifts to a higher wavenumber. It is important to note that with an
increasing R value the intensity of the shifted peak decreases
considerably. At approximately R= 2.8 to R= 3.2 these additional
bands have essentially disappeared, again. This intensity decrease
seems to be consistent with the decrease in the number of DMSO
molecules solvating zinc cation.

d) *150 to 230 cm^{-1} region of the Raman spectra.*

The fourth region contains the vibrations due to the zinc
bromide complexes as a whole (Figure 4). These original spectra
contain an exponential background due to the Rayleigh scattering.
This background was subtracted by using an exponential-quadratic
base-line correction program (22,23), to give Figure 5.

Three Raman bands at 197, 180 and 166 cm^{-1} corresponding to
zinc bromide complexes are clearly seen in Fig.5. At the low R
values the presence of an additional band is also expected at 207
cm^{-1}. (A very weak shoulder at ~ 176 cm^{-1} for R=1.0 (Fig.4)
corresponds to a band of the hexasolvate observed by Sandström et
al. (6)). The band at 166 cm^{-1} is detected only for R > 3.2. These
four bands seem to be related to four complexes: $ZnBr^+$, $ZnBr_2$,
$ZnBr_3^-$, and $ZnBr_4^{2-}$. Ahrland et al. have reported the presence of
three complex species — $ZnBr^+$, $ZnBr_2$, and $ZnBr_3^-$ (7,8) — and have

calculated their formation constants from calorimetric data. When the concentrations of the species are calculated using their formation constants, it is proposed that the dominant species at R=3.2 is $ZnBr_3^-$; this proposal is consistent with the fact that the Raman spectrum has only one peak at 180 cm^{-1} for the R=3.2 sample (Figs.4 and 5). This fact allows an identification of the bands as follows: 207 ($ZnBr^+$), 197 ($ZnBr_2$), 180 ($ZnBr_3^-$), and 166 cm^{-1} ($ZnBr_4^{2-}$). The obvious appearance of the 166 cm^{-1} peak at R > 3.2 confirms the existence of the $ZnBr_4^{2-}$ complex.

In order to isolate the spectrum of each species from the overlapped spectra, factor analysis was applied to this spectral region after base-line correction. It was difficult to obtain the absolute intensities of each spectrum from experiments. Thus all spectra were normalized assuming the intensity at 180 cm^{-1} to be constant (See Figure 5): $ZnBr_3^-$ standard. The procedure for the factor analysis is described in Appendix A. The analysis showed that three or four factors are necessary to reproduce the measured spectra. The indication of four factors (four complexes) was adopted, as this is consistent with the existence of four bands described above. In this case, the spectra shown by the dotted lines in Fig.5 were reproduced and are in good agreement with the measured spectra as shown by solid lines in Fig.5.

The extracted spectra of each pure species and their concentration distributions are shown in Figure 6. The spectrum of Factor A and that of Factor D show some negative Raman intensities; and this fact indicates that this result is not necessarily correct. In factor analysis, many combinations of spectra and concentration distributions, namely **R** and **C** matrices (being introduced in Appendix A), reproduce the same spectral data (**I**). We can rotate

the bases of these two matrices **R** and **C**, while keeping their
product **I** constant. In order to carry out a meaningful rotation of
the matrix, we adopted a new method, called Factor Analysis with
Equilibria Constraints (FAEC) described in Appendix B, which took
into account information about the equilibria among species. As a
result, the spectrum of each species and its concentration change as
shown in Figure 7 were obtained. The spectra of Factors A and D
still have a large contribution from the noise component, but no
longer have any significant negative intensity. The formation
constants were also obtained by the treatment of Appendix B and are
tabulated in Table 2, together with the values determined
calorimetrically (4-7). The calorimetric results suggested that the
formation constants depend strongly on the ionic media; for example,
in the case of 1M NH_4^+, interaction between NH_4^+ and Br^- is

expected. Recognizing such dependence upon the solution composition,
the formation constants obtained in this work are fairly consistent
with the others. Our analysis does not lead to precise estimates of
the errors associated with the formation constants, other than the
goodness of fit to the original spectra (Fig.5). Considering errors
in baseline construction and signal noise, uncertainties of +10%
would not be unreasonable. Raman spectroscopy is particularly
valuable for identifying species and equilibria but lacks the
precision available from such methods as potentiometry for
quantitative analysis.

Distribution curves for each species are shown in Fig. 8.
In the upper panel of Fig.8, the fractions of each species are
plotted versus logarithmic values of the free bromide concentration.
Nine vertical lines show the corresponding positions of log $[Br^-]$ of
the sample solutions used for this work, labelled with each R value.
The figure indicates that the predominant equilibrium is between

ZnBr$_2$ and ZnBr$_3^-$ in the range from R= 2.4 to 3.2. On the other hand, when log [Br] > -1, namely [Br] > 0.1, the contribution from the species ZnBr$_4^{2-}$ becomes important. Ahrland et al. reported that ZnBr$_4^{2-}$ is negligible; it was not required in the previous interpretation of the calorimetric data (7,8). Our results, however, positively suggest the presence of ZnBr$_4^{2-}$. This ion is well characterized in aqueous solutions (20,24).

Ahrland et al. have concluded that the complex with two or more bromide ions is tetrahedral; but ZnBr$^+$ might be octahedral in some ionic media (7,8). The ~15 cm^{-1} equi-interval shift of Raman bands of successive zinc bromide complexes to lower wavenumbers, as shown in Fig.7, may suggest that the four complex species have the same coordination; thus ZnBr$^+$ may also be a tetrahedral ion, and only the Zn^{2+} solvated ion is octahedral. The concept that ZnBr$^+$ has tetrahedral coordination is consistent with the earlier report of Ahrland, carried out in 1M NH$_4$ClO$_4$ media (4).

The lower panel of Fig.8 gives the calculated result for the fraction of DMSO molecules solvating zinc ion plotted versus log [Br$^-$], assuming that free Zn^{2+} ion has octahedral solvation and all zinc bromide complexes have tetrahedral coordination. The amount of DMSO octahedrally solvating zinc ion, DMSO$_{O_h}$ of Fig.8, rapidly decreases and becomes almost zero at R=2.8. The total amount of DMSO molecules tetrahedrally solvating zinc ion, DMSO$_{T_d}$ of Fig.8, increases with the increase of the R value. Comparing Fig.2 and Fig.3 with the lower panel of Fig.8, the following picture can be imagined: the DMSO which is responsible for the shifted Raman bands, the shaded parts of Fig.2 and Fig.3, is octahedrally solvating the 'free' zinc ion, not the tetrahedral species. Thus,

the shaded parts disappear about R=2.8. This opinion is still speculative, but seems to be reasonable when we consider that any zinc bromide complex has a less positive central charge due to the effect of the negative charge on the attached bromide; and an effective attraction for the electrons of DMSO by the complex becomes weaker than in the case of the di-charged free zinc ion. It is also worth noting that the nexaaquozinc ion gave a Raman signal, but not the bromide-containing complexes (20). Equilibria among Zn^{2+}, $ZnBr^+$, $ZnBr_2$, $ZnBr_3^-$, and $ZnBr_4^{2-}$ explain all the properties of the Raman spectra observed for DMSO solutions.

In conclusion, the Raman spectra of DMSO solutions containing zinc bromide complexes give information about the stepwise formation of the zinc bromide complexes as well as information about the structure arising from the solvating DMSO molecules.

Appendix A General procedure of Factor Analysis

Factor analysis is a powerful procedure for the analysis of overlapped spectra (25-28). A data matrix **I** is formed from the Raman intensities; in this work nine solutions were prepared and the intensities of 80 wavenumber points were used for each spectrum. All spectra used were normalized at 180 cm^{-1} so as to have constant intensity. The data matrix **I** consists of 80 rows and 9 columns. Each column corresponds to the intensity -normalized (at 180 cm^{-1}) spectrum of each sample solution. A second-moment matrix (sometimes called covariance matrix) **Z** is obtained by multiplication of the data matrix **I** with its transposed matrix ^{t}**I**.

[1]   **Z**   = ^{t}**I** **I**

Using the Jacobi method, an eigenvalue matrix **E** and an eigenvector matrix **Q** are obtained.

[2] $$Z = {}^tQ \ E \ Q$$

The eigenvalue matrix **E** will have the same number of rows as **Z**. The number of independent components in the sample spectra, NC, can be obtained from the *IND* function introduced by Malinowski (29) or by checking the original data matrix **I** with the reproduced data matrix **I'** assuming a proper number of NC.

In the case of NC factors, the eigenvectors corresponding to the NC largest eigenvalues can be taken out and aligned in rows to construct a new matrix **C**, known as the first expression for the concentration matrix. By multiplying the transpose of the concentration matrix **C** with the data matrix **I** a new matrix **R** is obtained, which is known as the spectral matrix.

[3] $$R = I \ {}^tC$$

When the spectral matrix **R** is multiplied with the concentration matrix **C**, a theoretical data matrix is reproduced.

[4] $$I' = R \ C$$

The reproducibility of the theoretical data matrix can be examined by calculating the error function *ER* , which is the sum of the squares of the differeces of each element of two matrices **I** and **I'** (25).

[5] $$ER = (\Sigma_i \Sigma_j \ ((I)_{ij} - (I')_{ij})^2)^{1/2} / (\Sigma_i \Sigma_j ((I)_{ij})^2)^{1/2}$$

where $(I)_{ij}$ indicates the element at i^{th} row and j^{th} column of the matrix **I**. The optimum number of factors, NC, can be selected as the number where convergence of *ER* is observed.

In this work *IND* function proposed the presence of three factors; and *IND* function proposed three or four factors as independent factors. From the discussion of the number of complexes in the sample solutions (see text), factor number NC = 4 was adopted. The result from the *IND* function simply implies that

the contribution of the peak at 207 cm^{-1} ($ZnBr^{+}$) to the observed Raman spectra is very small. As a result, a spectral matrix **R** of 80 rows and four columns, and a concentration matrix **C** of four rows and nine columns were obtained. Each column of **R** corresponds to the spectrum of each constituent as shown in Fig.6, and each row of the concentration matrix **C** corresponds to a concentration distribution of this constituent.

Appendix B Rotation of bases of R and C based on the equilibria among the species. -- Application of FAEC (Factor Analysis with Equilibrium constraints) --

The **R** and **C** matrices sometimes contain negative values. The result of Appendix A is such a case. Now the bases of matrices can be rotated to avoid such negative values.
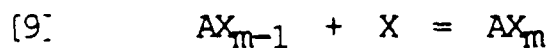
[6] $\qquad R^{O} \quad = \quad R \ T_R$

[7] $\qquad C^{O} \quad = \quad T_C \ C$

If the rotation matrices T_R and T_C have the following relationship,

[8] $\qquad T_R \ T_C \quad = \quad U$

where **U** is the unit matrix having unit value as diagonal elements and zero value as other elements, the product of R^{O} and C^{O} remains exactly the same as **I'** (Eq. [4]).

We assume the following equilibrium reaction for the stepwise zinc bromide complex formation:

[9] $\qquad AX_{m-1} + X = AX_m$

Then, we can express the stepwise formation constant K_m as follows,

[10] $\qquad K_m \quad = \quad [AX_m] \ / \ [AX_{m-1}] \ [X]$

where the relation between the cumulative stability constant β and the stepwise formation constant K_m is expressed as follows,

[11] $\qquad \beta \quad = \quad K_1 \ K_2 \cdots K_m$

In this work, we assume the presence of four zinc bromide complexes; thus we have four K's. If the values of K's and the total amount of the reagents (zinc ion and bromide ion) are known, the real concentration of each species in each solution, which corresponds to the elements of the true concentration matrix C^O, can be calculated assuming the activity coefficients are unity. The matrix obtained from factor analysis, C, can be related to this C^O by using the proper rotation matrix T_C through Eq. [7]. The elements of the rotation matrix, T_C, can be obtained by applying the nonlinear least squares method to minimize the following function LSM (30).

[12] $\qquad LSM = \sum_i \sum_j ((C^O)_{ij} - (T_C\ C)_{ij})^2$

A set of K values gives one LSM value. By iterative refinement of K values so as to give a minimum LSM value, finally an optimum set of $K's$ and T_C is obtained. Thus the optimum matrices C^O and R^O are also obtained using Eq. [6]-[8]. As a result, this procedure produced the spectra and the concentration distributions as shown in Fig. 7, as well as a set of formation constants as tabulated in Table 2. For initial values of the parameters, K's , the literature values of Ahrland and Persson were used (8).

REFERENCES

1. S. Ahrland and N.-O. Björk. *Acta Chem. Scand.* **A30**, 249 (1976).

2. S. Ahrland and N.-O. Björk. *Acta Chem. Scand.* **A30**, 257 (1976).

3. S. Ahrland and N.-O. Björk. *Acta Chem. Scand.* **A30**, 265 (1976).

4. S. Ahrland, N.-O. Björk, and R. Portanova. *Acta Chem. Scand.* **A30**, 270 (1976).

5. S. Ahrland, L. Kullberg, and R. Portanova. *Acta Chem. Scand.* **A32**, 251 (1978).

6. M. Sandström, I. Persson, and S. Ahrland. *Acta Chem. Scand.* **A32**, 607 (1978).

7. S. Ahrland, N.-O. Björk, and I. Persson. *Acta Chem. Scand.* **A35**, 67 (1981).

8. S. Ahrland and I. Persson. *Acta Chem. Scand.* **A35**, 185 (1981).

9. I. Persson. *Pure and Appl. Chem.* **58**, 1153 (1986).

10. W.D Horrocks, Jr. and F.A. Cotton. *Spectrochim. Acta*, **17**, 134 (1961).

11. M.-T. Forel and M. Tranquille. *Spectrochim. Acta*, **26A**, 1023 (1970).

12. S. Itoh and H. Ohtaki. *Z. Naturforsch*, **42A**, 858 (1987).

13. W. Bol, G.J.A. Gerritis, and C.L. van Panthaleon van Eck. *J. Appl. Crystallogr.* **3**, 486 (1970).

14. G. Johansson. *Acta Chem. Scand.* **25**, 2787 (1971).

15. G.E. Maciel, L. Simeral, and J.J.H Ackerman. *J. Phys. Chem.* **81**, 263 (1977).

16. T. Drakenburg, N.-O. Björk, and R. Portanova. *J. Phys. Chem*, **82**, 2423 (1978).

17. H. Ohtaki and G. Johansson. *Pure and Appl. Chem.* **53**, 1357 (1981).

18. W.Yellin and R.A.Plane. *J.Am.Chem.Soc.* **83**, 2448 (1961).

19. D.E. Irish. in *Ionic Interactions*, Edited by S. Petrucci. Academic, New York 1971. Chap.9. p.187.

20. M.M. Yang, D.A. Crerar, and D.E.Irish. *J.Solution Chem.* **17**, 751 (1988).

21. B.G. Anderson and D.E.Irish. *J.Solution Chem.* **17**, 763 (1988).

22. J.T.Bulmer, D.E.Irish, F.W.Grossman, G.Herriot, M.Tseng, and A.J.Weerheim. *Appl. Spectrosc.* **29**, 506 (1975).

23. K.Murata and D.E.Irish. *Bunseki Kagaku*. **36**, T72 (1987).

24. P.L. Goggin, G. Johansson, M. Maeda, and H. Wakita. *Acta Chem. Scand.* **A38**, 625 (1984).

25. E.R. Malinowski and D.G.Howery. *Factor Analysis in Chemistry*; Wiley: New York, (1980).

26. T. Ozeki, H. Kihara, and S. Hikime. *Bunseki Kagaku*, **35**, 885 (1986).

27. T. Ozeki, H. Kihara, and S. Hikime. *Anal. Chem.* **59**, 945 (1987).

28. T. Ozeki, H. Kihara, S. Hikimie, and S. Ikeda. *Anal. Sci.* **3**, 285 (1987).

29. E.R. Malinowski. *Anal.Chem.* **49**, 612 (1977).

30. T.Ozeki, H.Kihara, and S.Ikeda. *Anal. Chem.* **60**, 2055 (1988).

Table 1 Analytical Compositions of Nine Sample
solutions with Different R Values.

R	Zn^{2+}	Br^-	Na^+	ClO_4^-
1.0	0.649	0.649	0.000	0.649
1.5	0.786	1.178	0.000	0.394
2.0	0.484	0.968	0.000	0.000
2.4	0.517	1.241	0.207	0.000
2.8	0.496	1.389	0.397	0.000
3.2	0.466	1.492	0.560	0.000
3.6	0.294	1.058	0.470	0.000
4.0	0.406	1.624	0.812	0.000
6.0	0.169	1.016	0.678	0.000

Table 2 Stepwise Stability Constants of Zinc
Bromide Complexes in DMSO.

	1M NH_4^+	0.1M NH_4^+	1M Na^+	This work
$\log K_1$	0.85	1.86	1.56	1.6
$\log K_2$	2.89	3.31	3.11	3.2
$\log K_3$	1.35	1.98	2.05	2.2
$\log K_4$	——	——	——	-0.6

Figure captions

Fig. 1   The 260 to 420 cm^{-1} region of the Raman spectra of samples with the specified values of R.

Fig. 2   The 800 to 1150 cm^{-1} region of the Raman spectra of samples with the specified values of R. Dotted lines are Raman spectra of pure DMSO solvent. The shaded part is the difference between the spectrum of the sample and that of pure DMSO.

Fig. 3   The 600 to 750 cm^{-1} region of the Raman spectra of samples with the specified values of R. Dotted lines are Raman specta of pure DMSO solvent. The shaded part is the difference between the spectrum of the sample and that of pure DMSO.

Fig. 4   The 150 to 230 cm^{-1} region of the Raman spectra of samples with the specified values of R.

Fig. 5   Comparison of normalized Raman spectra (solid line) and reproduced spectra (dotted line) from factor analysis.

Fig. 6   The Raman spectrum of each species and its concentration distribution obtained from factor analysis.

Fig. 7   The Raman spectrum of each species and its concentration distribution obtained after applying the equilibrium constraints among species.

Fig. 8   The calculated concentration distribution of zinc-containing species (upper figure) and the fractions of DMSO molecules solvating the zinc-containing species (lower figure).
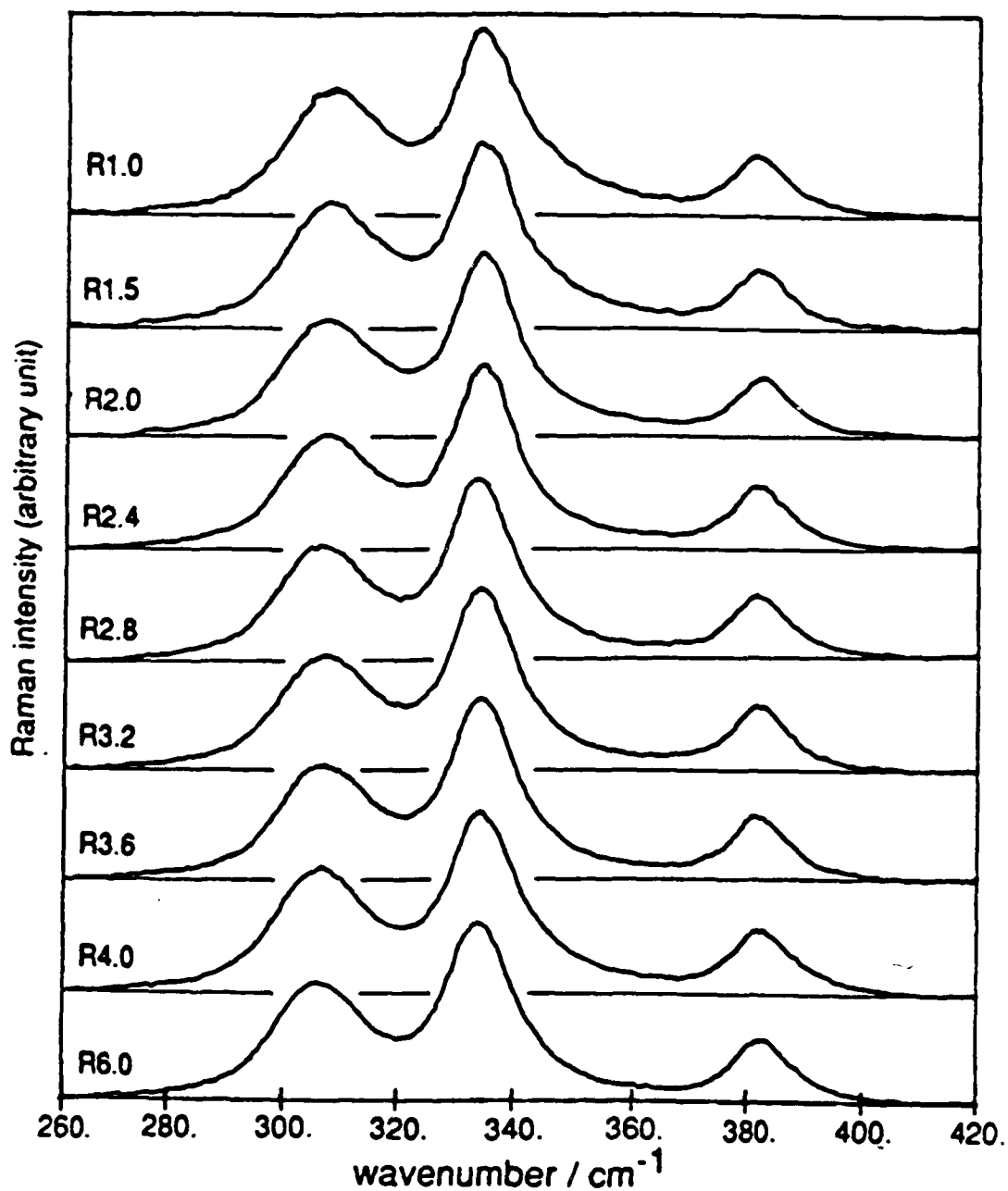
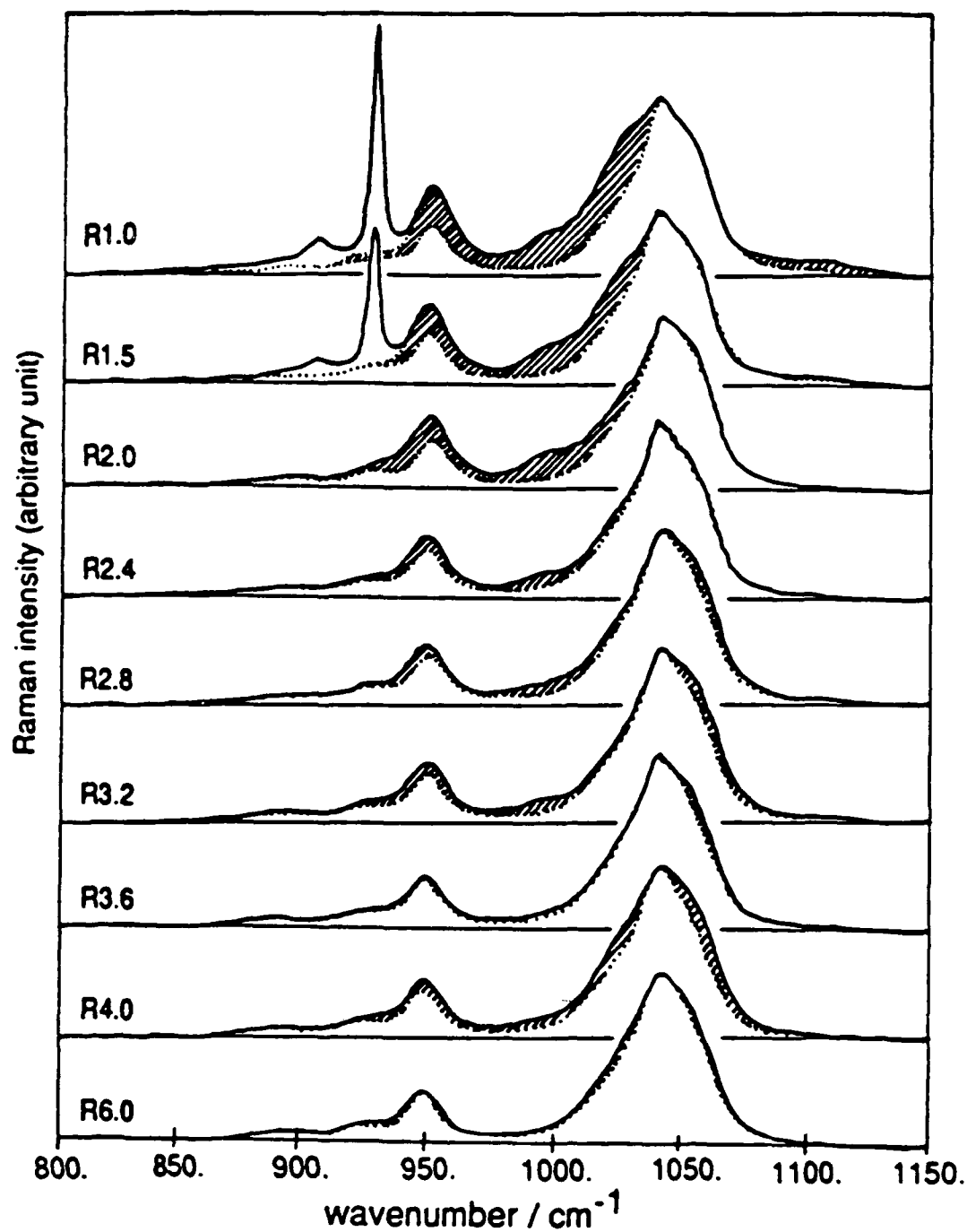Fig. 1   The 260 to 420 cm^{-1} region of the Raman spectra of samples with the specified values of R.

Fig. 2 The 800 to 1150 cm⁻¹ region of the Raman spectra of samples with the specified values of R. Dotted lines are Raman spectra of pure DMSO solvent. The shaded part is the difference between the spectrum of the sample and that of pure DMSO.
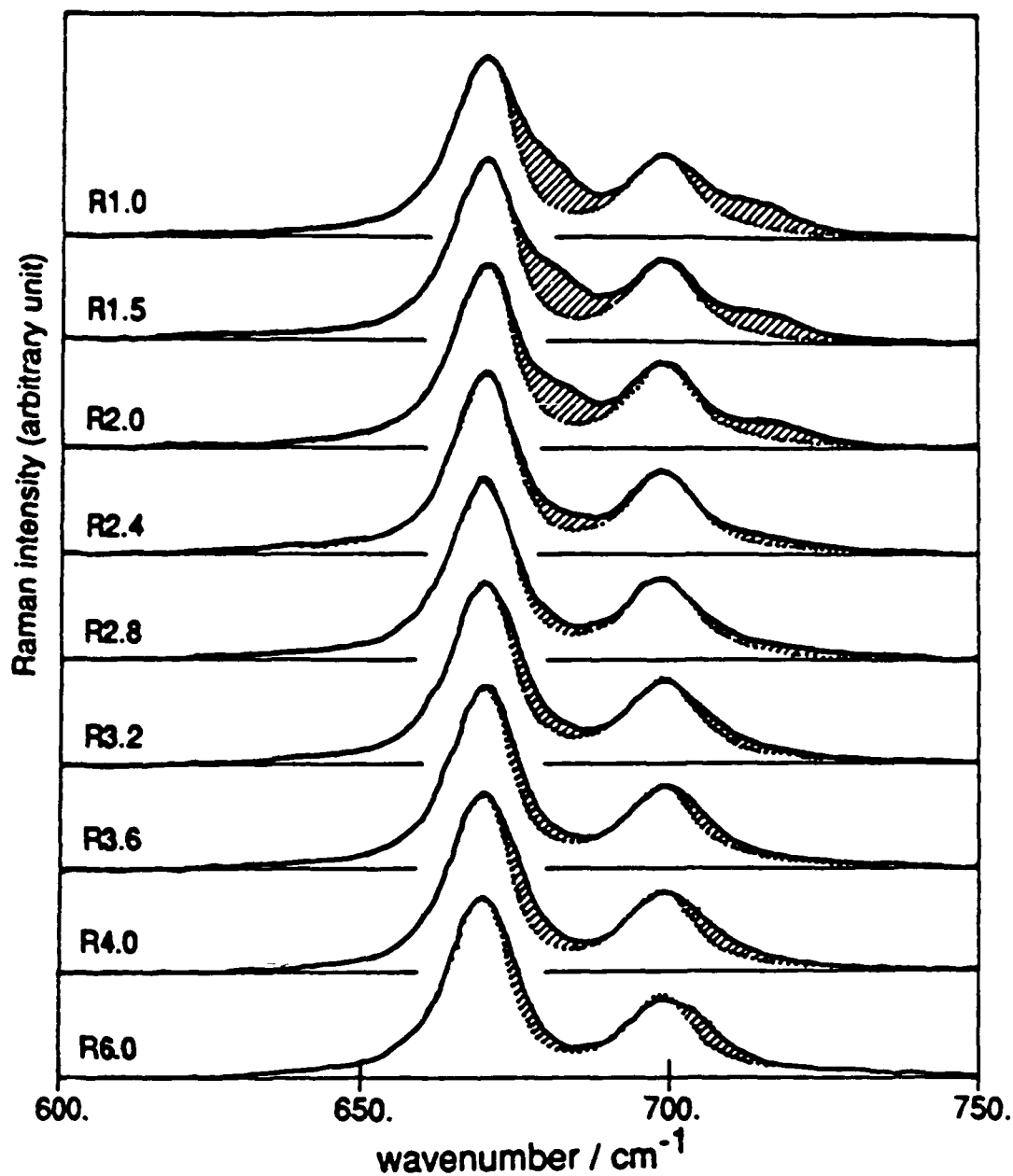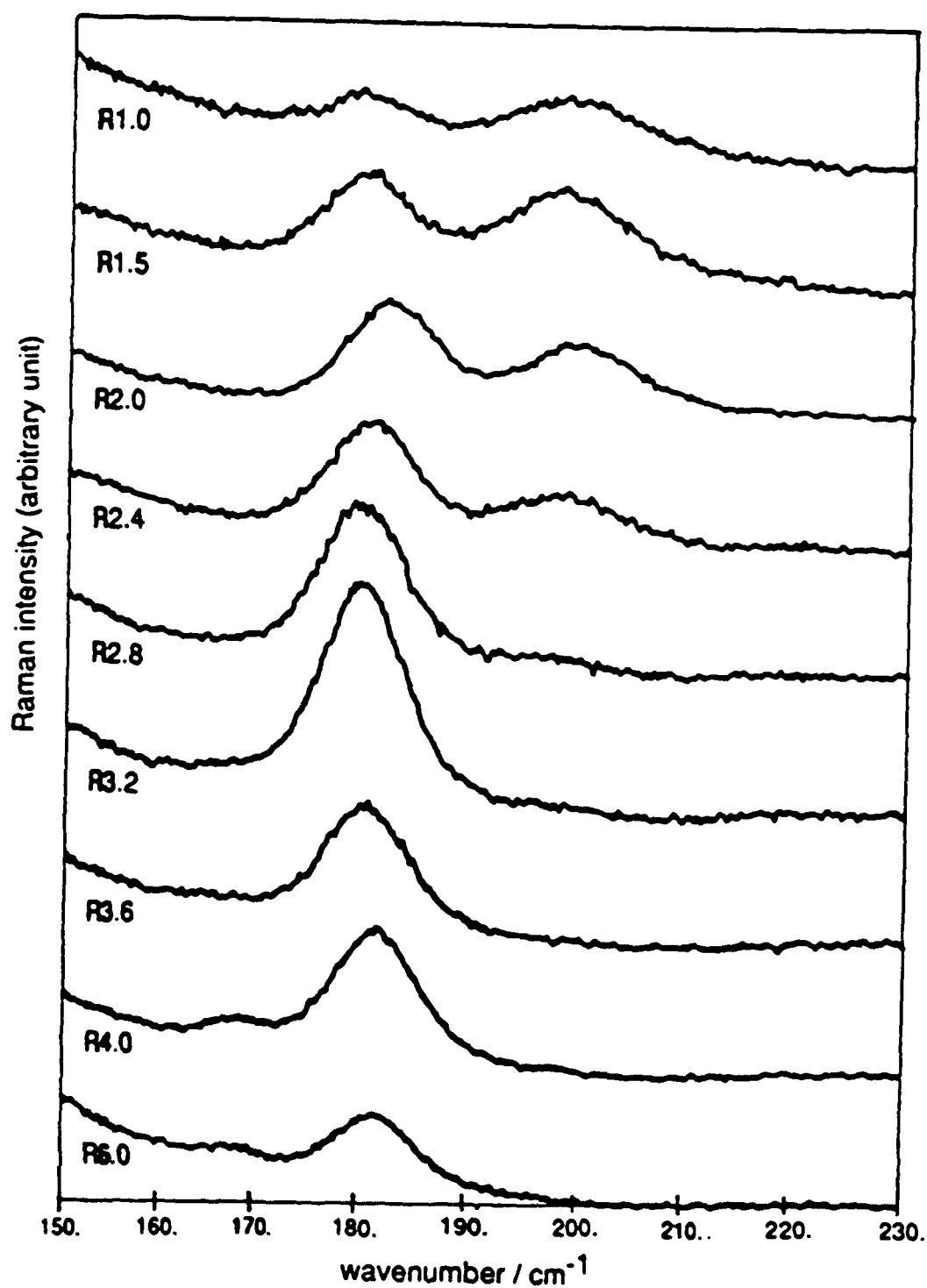
Fig. 3   The 600 to 750 cm^{-1} region of the Raman spectra of
samples with the specified values of R. Dotted lines are
Raman specta of pure DMSO solvent. The shaded part is the
difference between the spectrum of the sample and that of
pure DMSO.

Fig. 4 The 150 to 230 cm^{-1} region of the Raman spectra of samples with the specified values of R.
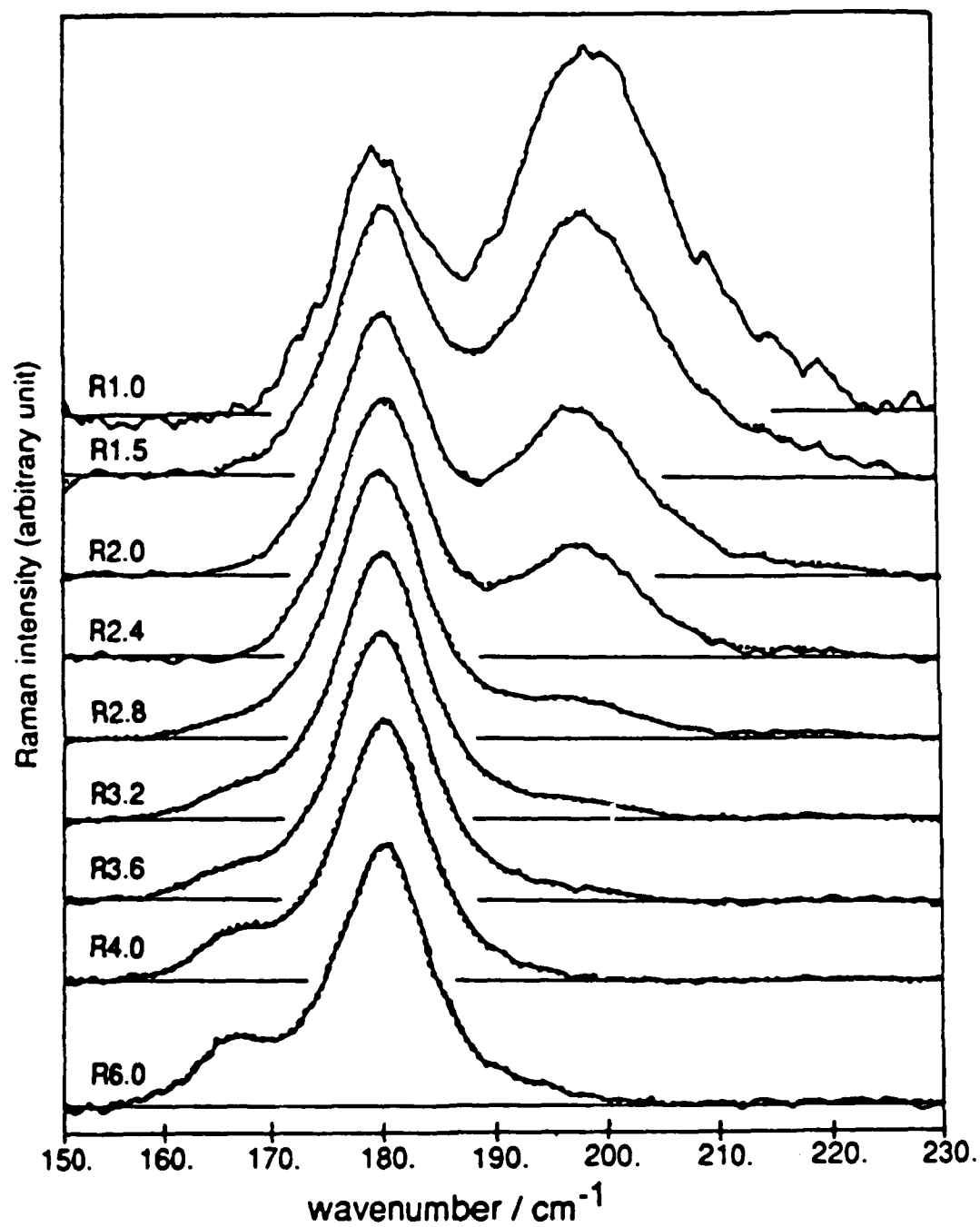
Fig. 5 Comparison of normalized Raman spectra (solid line) and reproduced spectra (dotted line) from factor analysis.
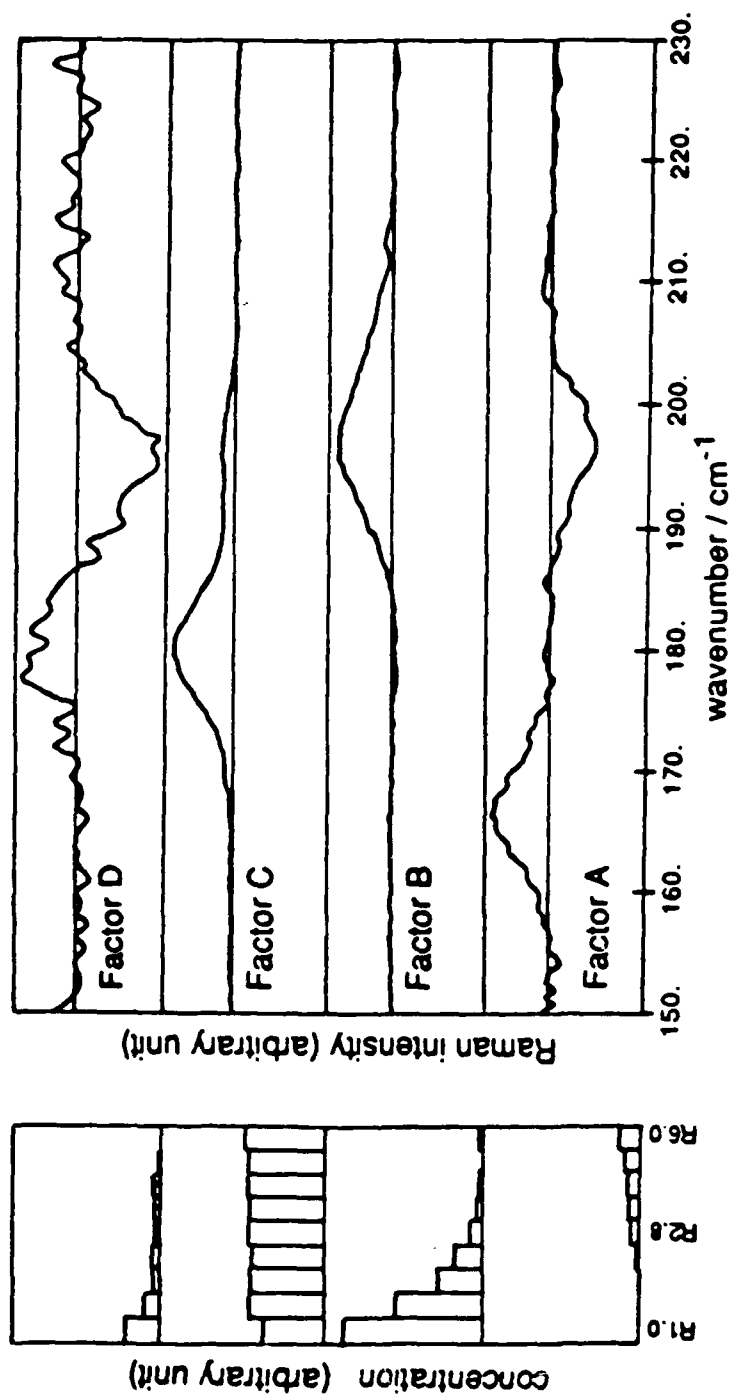
Fig. 6

Fig. 6   The Raman spectrum of each species and its concentration
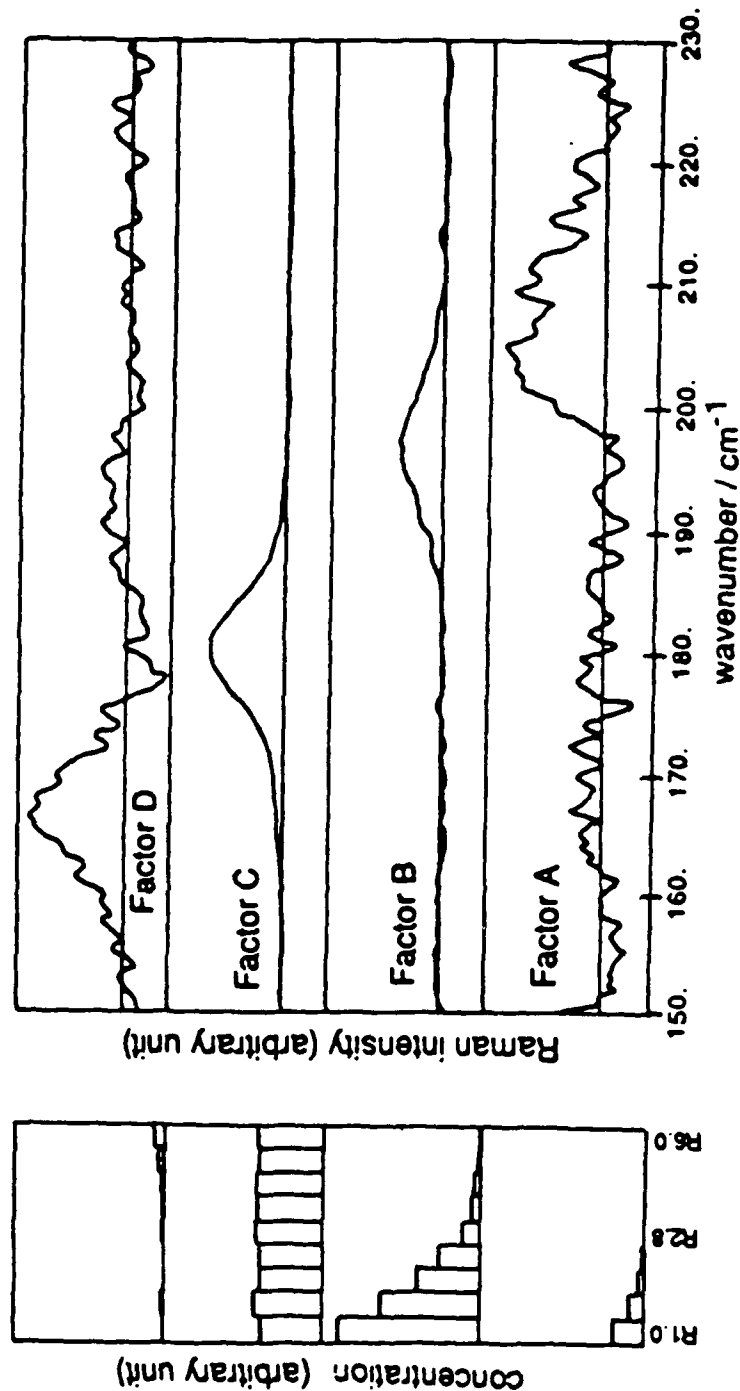
Fig. 7

Fig. 7　The Raman spectrum of each species and its concentration distribution obtained after applying the equilibrium constraints among species.
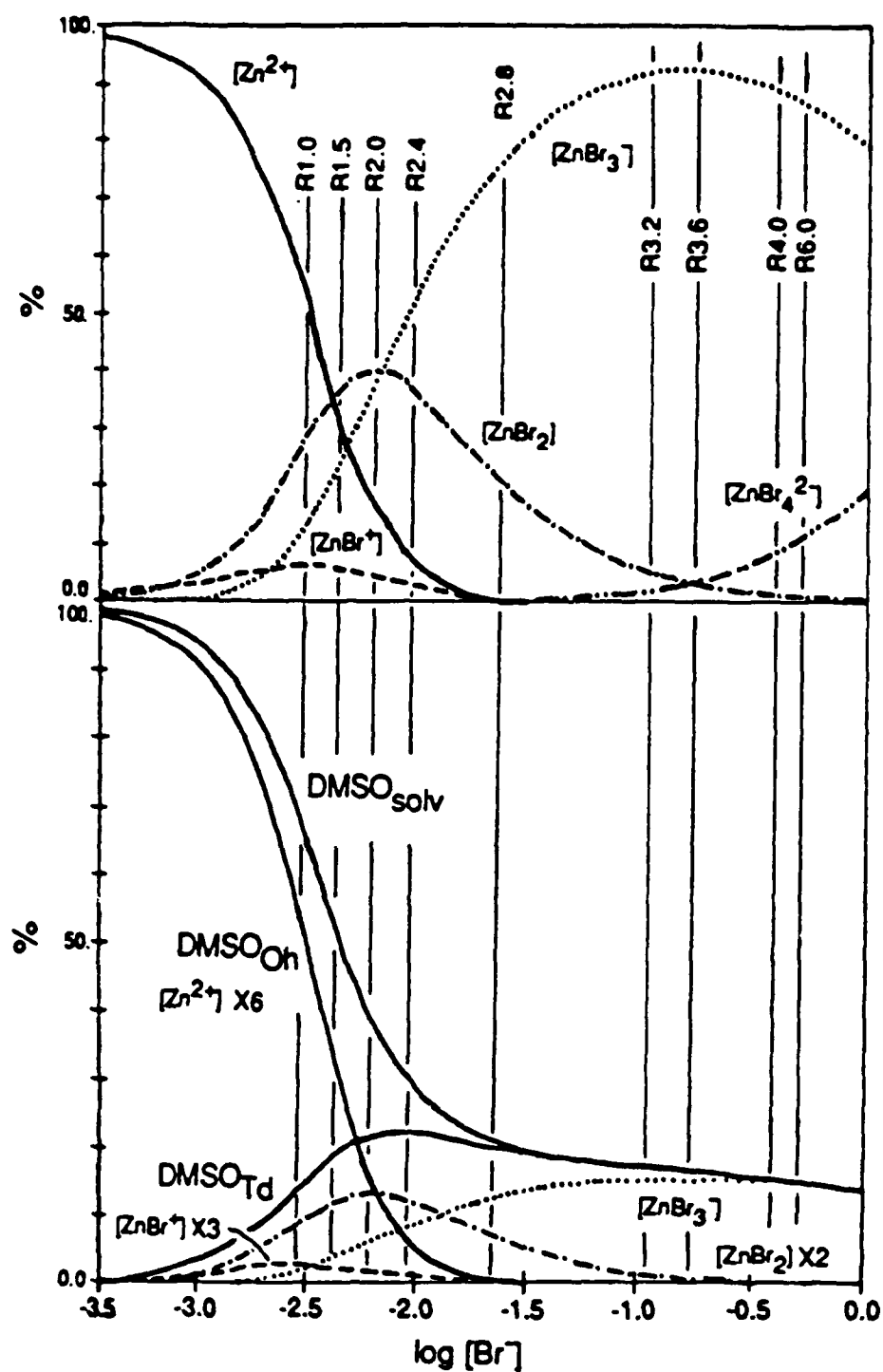
Fig. 8   The calculated concentration distribution of
          zinc-containing species (upper figure) and the fractions
          of DMSO molecules solvating the zinc-containing species
          (lower figure).

TECHNICAL REPORT DISTRIBUTION LIST, GEN

	No. Copies		No. Copies
Office of Naval Research Attn: Code 1113 800 N. Quincy Street Arlington, Virginia 22217-5000	2	Dr. David Young Code 334 NORDA NSTL, Mississippi 39529	1
Dr. Bernard Douda Naval Weapons Support Center Code 50C Crane, Indiana 47522-5050	1	Naval Weapons Center Attn: Dr. Ron Atkins Chemistry Division China Lake, California 93555	1
Naval Civil Engineering Laboratory Attn: Dr. R. W. Drisko, Code L52 Port Hueneme, California 93401	1	Scientific Advisor Commandant of the Marine Corps Code RD-1 Washington, D.C. 20380	1
Defense Technical Information Center Building 5, Cameron Station Alexandria, Virginia 22314	12 high quality	U.S. Army Research Office Attn: CRD-AA-IP P.O. Box 12211 Research Triangle Park, NC 27709	1
DTNSRDC Attn: Dr. H. Singerman Applied Chemistry Division Annapolis, Maryland 21401	1	Mr. John Boyle Materials Branch Naval Ship Engineering Center Philadelphia, Pennsylvania 19112	1
Dr. William Tolles Superintendent Chemistry Division, Code 6100 Naval Research Laboratory Washington, D.C. 20375-5000	1	Naval Ocean Systems Center Attn: Dr. S. Yamamoto Marine Sciences Division San Diego, California 91232	1

24